

Digital Image Correlation and Finite Element Analysis of Bone Strain Generated by Implant-Retained Cantilever Fixed Prosthesis

Keywords

Dental Implant
Finite Element Analysis
Biomechanical Complications
Computerized Models

Authors

João Paulo M. Tribst*
(DDS, MSc, PhD student)

Amanda M. O. Dal Piva*
(DDS, MSc, PhD student)

Marco Antonio Bottino*
(DDS, MSc, PhD, Professor)

Renato S. Nishioka*
(DDS, MSc, PhD, Professor)

Alexandre L. S. Borges*
(DDS, MSc, PhD, Professor)

Mutlu Özcan§
(DDS, MSc, PhD, Professor)

Address for Correspondence

Amanda M. O. Dal Piva*
Email: amodalpiva@gmail.com

* São Paulo State University (Unesp), Institute of Science and Technology, São José dos Campos, Brazil

§ University of Zurich, Dental Materials Unit, Center for Dental and Oral Medicine, Clinic for Fixed and Removable Prosthodontics and Dental Materials Science, Zurich, Switzerland

Received: 13.05.2019
Accepted: 09.09.2019
doi: 10.1922/EJPRD_1941Tribst08

ABSTRACT

Purpose: The present study evaluated the displacement and strain generated in an implant-supported fixed prosthesis under axial and non-axial loads using two methods. *Materials and Methods:* Three implants were inserted in a resin block. The Digital Image Correlation (DIC) was used to measure displacement and strain generated on the surface of the resin blocks for the different load applications (500N, 1 image/second). A 3-dimensional model was constructed and a load of 500 N was applied at an axial point and a non-axial point through finite element analysis (FEA). *Results:* Both methods gave similar trends for the strains, and both gave slightly higher strains with non-axial loading. FEA predicted higher strain magnitude ($\pm 11\%$) in comparison with DIC, but with the same mechanical behavior. According to ANOVA, the loading influenced the strain concentration. Higher strain was generated for non-axial loading around the implant nearest to the loading. *Conclusions:* For implant-retained cantilever fixed prosthesis, the same load applied in the lever arm induces higher strain in the cervical area of the last implant, which suggests more damaging potential than a load applied at the center of the prosthesis.

INTRODUCTION

Tooth rehabilitation consists of a complex theme in dentistry since the early loss of dental elements impacts directly on patients' quality of life.¹ The use of osseointegrated implants allows complex rehabilitations. However, mechanical problems can lead to changes in the stress distribution of the prosthesis/implant system,^{2,3} allowing the loss of osseointegrated implants and clinical complications, such as: the increasing of bone resorption, restoration failure or torque loss.¹

Since masticatory forces are directly transmitted to bone tissue, correct understanding of the biomechanics of this restorative modality is necessary.⁴ The principal biomechanical tools to investigate the strain in osseointegrated implants are finite element analysis (FEA), strain gauge (SG), photoelasticity and digital image correlation (DIC). The association of two or more methods allows a more reliable result and conclusions for the mechanical response in dental implants.⁴⁻¹⁰ Since load transmission in implant-supported fixed prosthesis can be directly influenced by the implant position and load direction,⁴ it is important to understand the mechanical response of cantilever prosthesis.⁹

The use of a cantilever prosthesis appears to be an easy solution when it is necessary to replace a tooth in regions without support. However, few studies on the biomechanics fields are available with experimental validation.¹¹⁻¹³ Benzing *et al.* (1995),¹² using finite element analysis and strain gauge methodology, concluded that spread-out implant arrangement to avoid cantilever restoration is better for bone stress concentration. Rubo *et al.*, (2010)¹³ using finite element analysis evaluated different implant-supported prosthesis and observed that the stress concentration was higher in the implants near the loading area and proportional to the cantilever length. Peixoto *et al.* (2017)¹¹ used DIC method to investigate the influence of veneering material and implant type on the strain distribution of implant-supported fixed partial dentures. The authors observed that conventional implants shows a better stress distribution than short implants.

DIC is a non-destructive method that has been introduced in dentistry studies to evaluate the strain distribution on the materials surface. It consists of an optical method of measuring the strain distribution during a mechanical test, through all surface differently from strain gauge analysis.⁵ For that, a series of images are captured using a camera and then analyzed

by a specific software through displacement of the surface points.⁶ After, the strain is calculated according to a derivation of the displacement fields (as with SG), but with the advantage of allowing a full surface view.^{5,6,11} The purpose of this study was to evaluate two clinical implant-supported fixed prosthesis scenarios: a centralized (axial) and a cantilevered loading (non-axial), using DIC and FEA.

MATERIALS AND METHODS

A graphical abstract of both methods is presented in Figure 1.

DIGITAL IMAGE CORRELATION (DIC)

For the bone tissue simulation in the experimental model, a bone block was fabricated from polyurethane resin (Polyurethane F160 Axson, Cergy, France) with dimensions of 95 x 45 x 30 mm (length, height and depth, respectively).^{4,9} After resin polymerization, the block had its surfaces polished with sandpapers (# 220 - # 600) (3M ESPE, St. Paul, USA) under constant water irrigation. For implant placement in the block, a set of milling cutters was used according to the manufacturer's

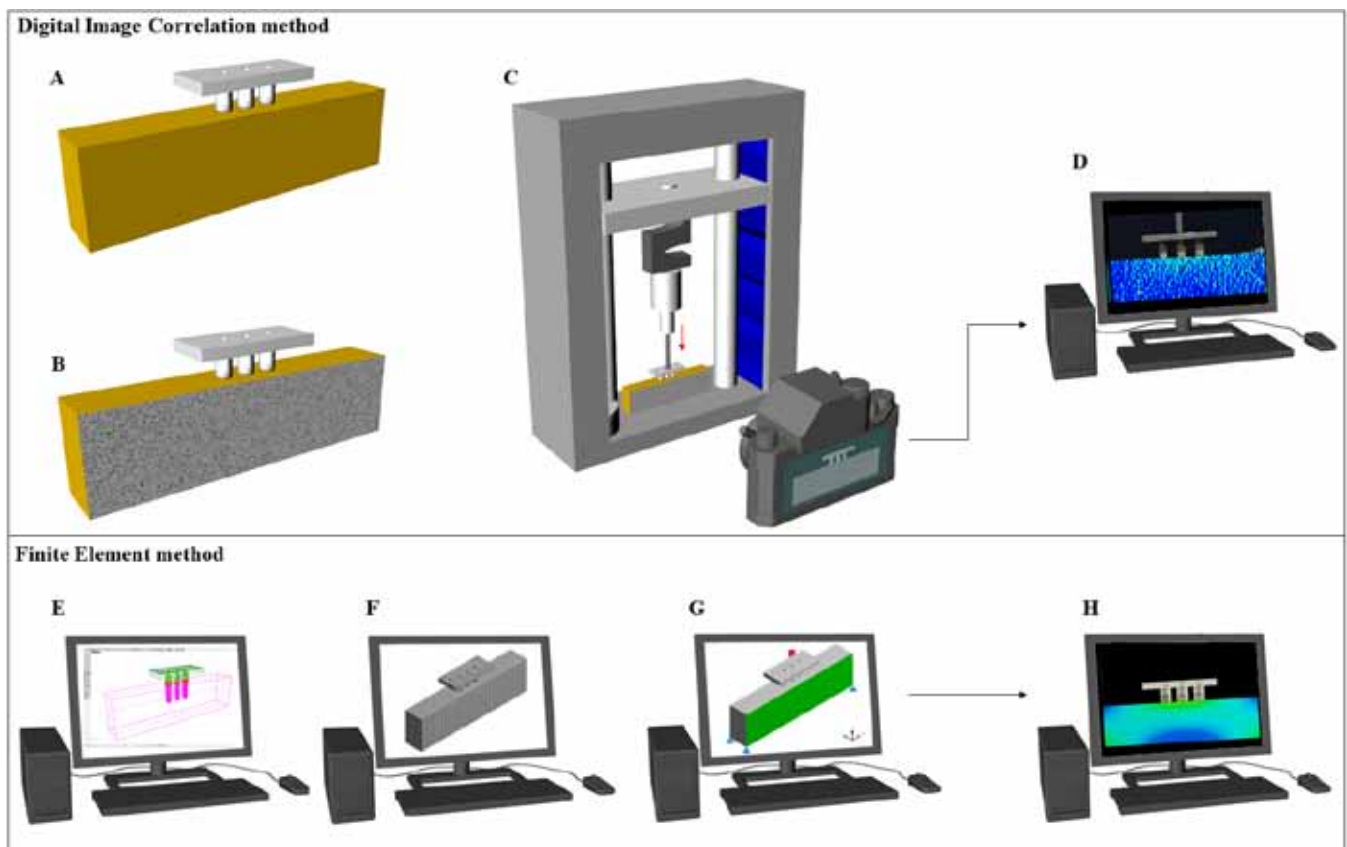


Figure 1: Graphical abstract of both performed methods to analyze the biomechanical behavior of 3-unit implant-supported prosthesis. For digital image correlation (DIC) an in vitro model was used as bone simulator with 3 implants (A). The buccal face of the model was discretized with painted dots (B). The model was submitted to an in vitro test in an universal testing machine while a camera recorded the images (C). The correlation of images displacement was converted in colorimetric graphs digitally (D). For the finite element method (FEA), the same sample was virtually modeled (E). In the analysis software, the model was meshed in a finite number of elements (F). The boundary conditions was manually determined following the in vitro test and the bone buccal surface was evaluated (G). The strain results were recorded in colorimetric maps (H).

recommendations (As Technology Titanium Fix, São José dos Campos, Brazil) and following the methodology used in previous studies.^{4,8} Three self-tapping external hexagon implants measuring 3.75 in diameter by 13 mm in length (As Technology Titanium Fix - São José dos Campos, Brazil) were linearly installed. Each implant received a corresponding number of installation sequence (Number 1 on the left side of the block, number 2 installed at the center of the block, number 3 on the right side of the block). Prosthetic abutments (Micro conical abutment) were installed on each implant with a torque of 20 N.cm with the aid of a torque wrench, following the manufacturer instructions. After placing the implants and abutments, a previously validated simplified fixed prosthesis was cast in CoCr alloy (Tilite Omega, Talladium Inc., USA) and installed with 10 N.cm under each abutment.⁹

The DIC technique was used to measure strains generated on the surface of the resin models for the different load applications.⁶ A professional camera (Canon EOS Rebel T5 with Tamron 90 mm f/2.8 SP VC AF Macro-Lens) was used for capturing the images of the deforming body and a specialist software package (Gom correlate, Vtech Consulting Ltda, São Paulo, Brazil) for subsequent image analysis. The camera had a resolution of 18.00 Megapixels. The surface of the resin model facing the camera lens was sprayed with a fine layer of white and black paint to produce irregular-shaped speckles for ease of tracking and analysis by the image correlation system.⁶ A static non-impact load of up to 500 N was applied using a universal testing machine (DL-1000, EMIC, São José dos Campos, Brazil) in two distinct moments: on the center of the framework axially to the implant center (implant 2); and in 5 mm of cantilever distally to the implant on the right (implant 3).⁴

To measure the generated strains on the model, surface images were taken at a frequency of 1 Hz⁶ until the 500 N load (arbitrary overload condition of the second molar area) was reached.¹² The first image was taken before the load was applied, and the remaining images were compared to the first image to calculate the displacements on the model surface. Surface strains were then calculated from the displacements using image correlation software (GOM Correlate, Braunschweig, Germany). The cervical regions of the three implants were selected to analyze the generated strains values. The strain distribution over the height of the resin block was analyzed for each region of interest (from 0 to 5 mm).¹¹ In order to

reveal the difference in strain distribution between the different configurations, the noise effect must be minimized. As a result, strain averaged over 4 pixels of 0.5 mm wide each were calculated for each vertical position along the block height. The strain measurement system was verified by repeating the measurement 3 times.^{6,11} The vertical and horizontal displacement (mm) and direct strains in the horizontal direction (ϵ_{XX}) were calculated and compared between the groups. The data was submitted to one-way analysis of variance (ANOVA) followed by Tukey test, all tests with $\alpha=5\%$.

FINITE ELEMENT ANALYSIS (FEA)

Three-dimensional FEA models based on the polyurethane model used in the experimental analysis (DIC method) were constructed using computer-aided design (CAD) software (Rhino version 5.0SR8; McNeel North America, Seattle, USA). The model was then transferred to Ansys Workbench 17.0 (Ansys Inc., Canonsburg, USA) for the numerical simulation. Mechanical properties (Young's modulus and Poisson's ratio) of the used materials are summarized in Table 1.^{9,13,14} All materials were assumed to behave elastically, isotropic and homogeneously.¹⁵ The loading configuration followed the same for the DIC analysis, i.e. with a static load of 500 N. The contacts for abutment/implants, implant/screw, screw/abutment were set as non-linear frictional contact (0.3 μm).¹⁶ All other interfaces, for example those between the implants and the polyurethane resin, were configured to be perfectly bonded.⁸ A geometrically linear static analysis was carried out. All the FEA models had similar mesh densities (0.3 mm each element) to ensure consistency and accuracy in the simulations for this study, with higher node density in the regions of interest (Mesh convergence test of 10%).^{4,9} The 3D models contained a total of 719,255 nodes with 411,921 quadratic tetrahedral elements. The aspect ratio of mesh metrics presented average of 1.88 with standard deviation of 0.9. Vertical and horizontal displacement (mm) and maximum principal strains were also calculated with the FEA method on the resin block for further comparison between the different groups in this study. After comparison of coherence between the experimental (DIC) and virtual method (FEA),⁶ the von-Mises stress of the three implants was calculated to predict failure region from these ductile solids.¹⁷

Table 1. Elastic Modulus (GPa) and Poisson's ratio from each simulated material used during the static structural analysis performed by the finite element method. All mechanical properties were inserted in the engineering data source in the analysis software

Material/Structure	Elastic Modulus (GPa)	Poisson's ratio
Titanium ¹³	110	0.33
CoCr ¹⁴	218	0.33
Polyurethane ⁹	3.6	0.30

RESULTS

The overall surface strain distributions determined by both techniques were very similar, as illustrated in Figures 2 and 3 for axial and non-axial load applications, respectively. As expected, compressive strains were found in the cervical region of the bone block, around implant 2 for axial loading, and around implant 3 for non-axial loading. Concentrated strains were also found by both methodologies on the top surface of the bone block immediately below the applied load. The displacement distribution and compressive strains are illustrated in Figure 4.

Both methods gave similar trends for the strains, and both gave slightly higher strains for the group with non-axial loading however, the FEA models predicted higher strain magnitude ($\pm 11\%$) in comparison to DIC. The data peak over the

entire region of interest as determined by both methods (DIC and FEA) for all conditions are presented in Figure 4. In order to validate the obtained theoretical results from both methodologies, the maximum strain data were plotted in bar graphs and compared. Considering the stress fields in the implants structure, Von-Mises stress revealed higher stress concentration in the implant under non-axial loading (Figure 5). Direct strains (%) measured for the regions of interest in the horizontal direction (ϵ_{XX}) are illustrated in Figure 6. The mean values and standard deviations between the first and second molars are shown in Table 2.

According to one-way ANOVA, the loading application influenced the generated strain. Significantly higher strain was generated around implant 3 for non-axial loading when compared to axial loading. Implant 2 did not show a difference for peri-implant strain peak according to the loading. Furthermore, implant 1 decreased the mean strain when submitted to the non-axial loading ($p < 0.05$).

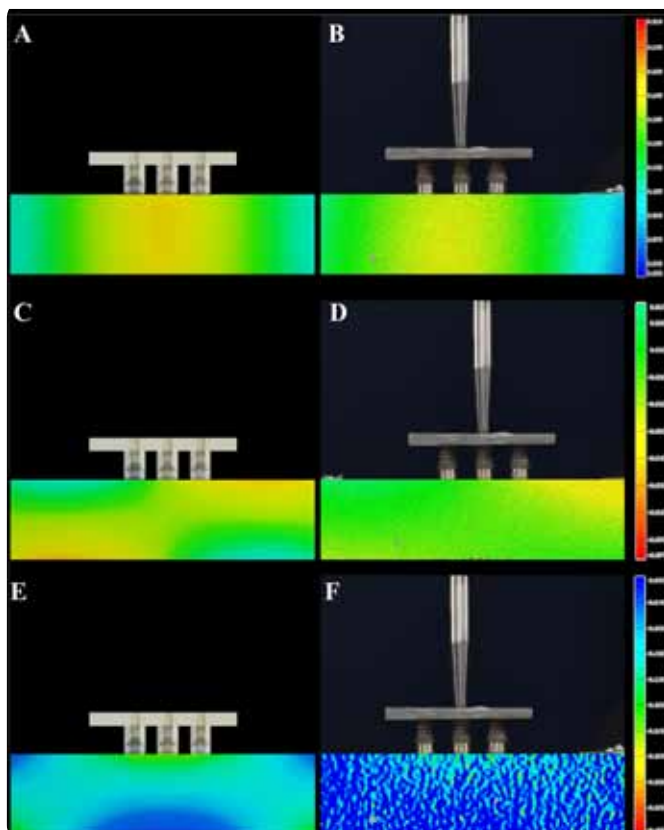


Figure 2: Comparison between the Finite Element Analysis – FEA (left column) and the Digital Image Correlation – DIC (right column) methods used to evaluate the stress distribution through an implant-retained cantilever fixed prosthesis submitted to an axial load (500N). From top to bottom, the results of Horizontal displacement, Vertical displacement and Compressive strains.

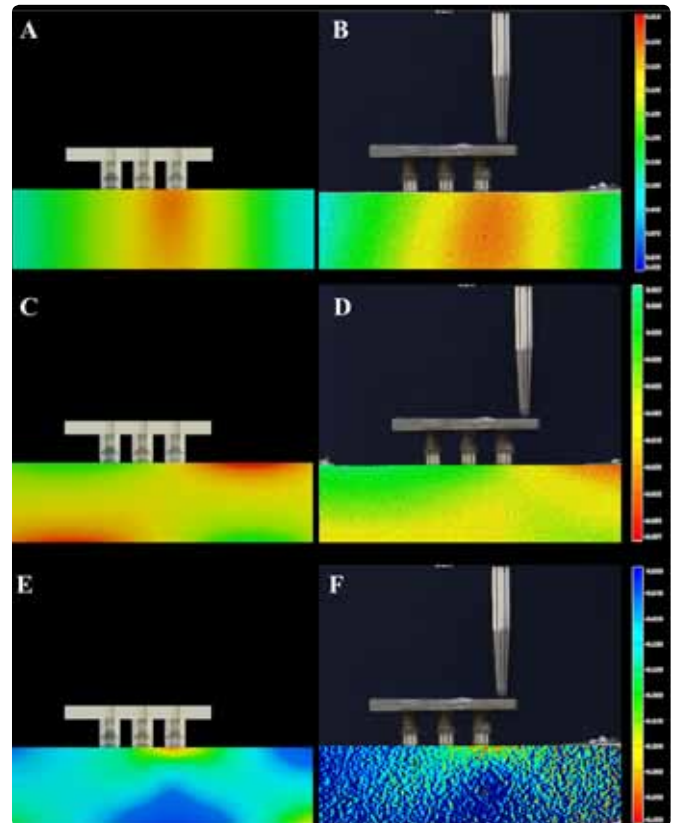


Figure 3: Comparison between the Finite Element Analysis – FEA (left column) and the Digital Image Correlation – DIC (right column) methods used to evaluate the stress distribution through an implant-retained cantilever fixed prosthesis submitted to a non-axial load (500N). From top to bottom, the results of Horizontal displacement, Vertical displacement and Compressive strains

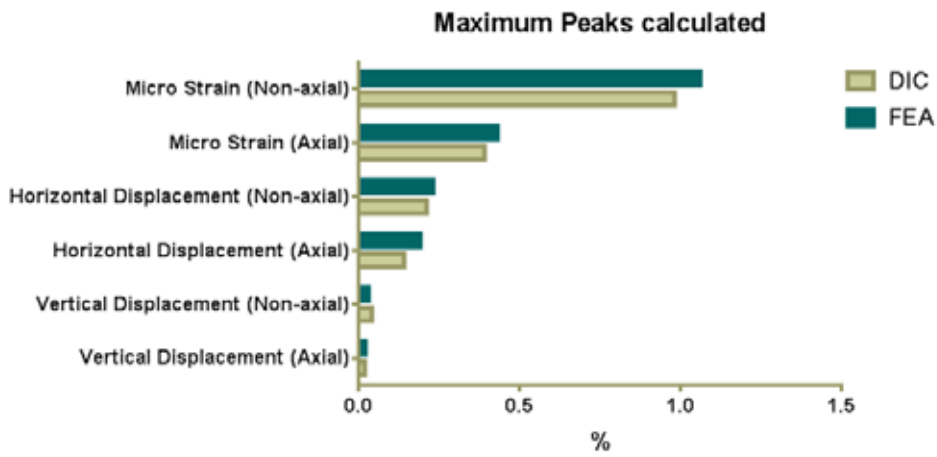


Figure 4: Horizontal and vertical displacement, and compressive strains maximum peaks for the two load application scenarios (axial and non-axial), using the two methods (DIC and FEA).

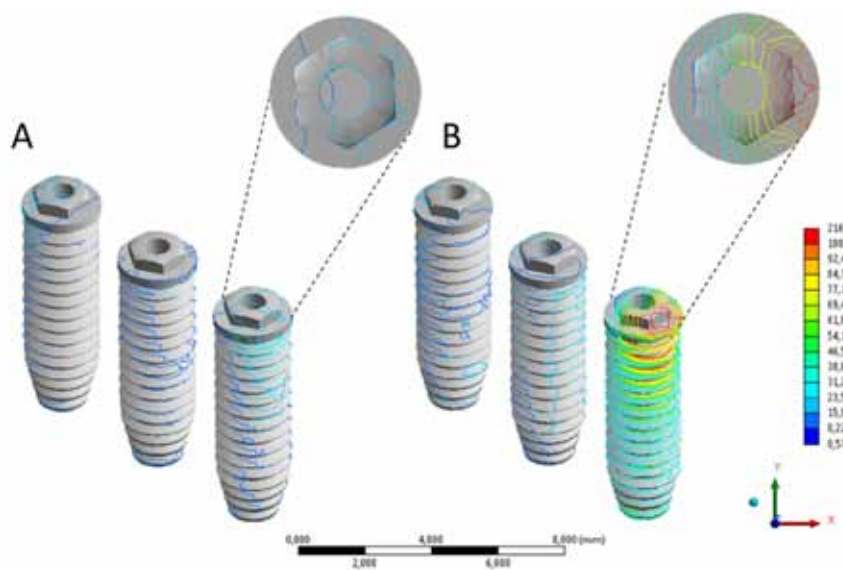


Figure 5: Isolines delimiting stress fields in the implants according to the results of Von-Mises stress. The results were obtained according to the applied load: A) axial and B) non-axial. Red color corresponds to higher stresses magnitude while the blue color corresponds to lower stresses concentration.

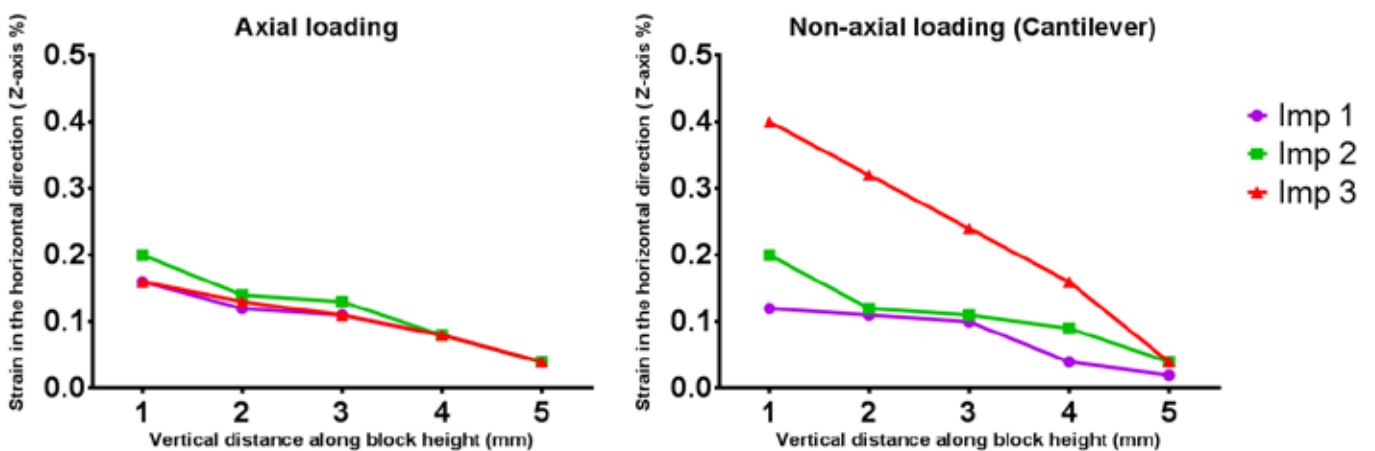


Figure 6: Compressive strains (eXX, %) at 5 mm from the cervical to the apex for each dental implant according to the applied load (axial and non-axial). Implant number 1 is on the left side of the block, number 2 was installed at the center of the block and number 3 is on the right side of the block.

Table 2. Digital Image correlation results. Microstrain mean \pm Standard deviation and Maximum Compressive Strain values (ϵ_{xx}) according to the applied load (axial and non-axial) and evaluated implant (Implant number 1 is on the left side of the block, number 2 was installed at the center of the block and number 3 is on the right side of the block).

Implant Number	Axial Loading		Non-axial Loading	
	Mean	Max	Mean	Max
1	-0.10 \pm 0.02 ^B	-0.16	-0.07 \pm 0.02 ^A	-0.12
2	-0.11 \pm 0.02 ^C	-0.22	-0.11 \pm 0.02 ^C	-0.22
3	-0.10 \pm 0.01 ^B	-0.16	-0.33 \pm 0.03 ^D	-0.39

Different capital letters for each implant indicate significant differences ($p < 0.05$)

DISCUSSION

In this study, DIC and FEA methods were employed to study the effects caused by an implant-supported fixed prosthesis under two load conditions: axial and non-axial. The results showed that the central implant did not present a significantly different peri-implant strain pattern under both loadings. The combination of an experimental model and a mathematical model for strain measurement is more reliable to provide an adequate interpretation of the collected results, avoiding conclusions based in non-valid models.^{6,8,9} It is visible that the *in silico* method (FEA) can provide results in geometries that cannot be easily analyzed by *in vitro* tests, as the stress distribution in the implant surface. But the correlation between both models (using the bone strain or another result if possible) is important to demonstrate that for this simulation, the biomechanical behavior present a convergent results. Preliminary comparisons between FEA and DIC methodologies suggested the direct evaluation of the theoretical and experimental strain pattern, comparing the strain maps qualitatively between both methods.^{6,7} The authors assumed that if the numerical model present a valid result similar to the *in vitro* behavior, the evaluation of internal stresses that cannot be measured during the *in vitro* method is possible.^{6,7} Based on this, the present study demonstrated with both methods that an implant-supported fixed prosthesis present an reduced strain magnitude with axial loading.

A block in polyurethane resin was used herein to simulate bone tissue. This material has already been defined in the literature as a valid isotropic material for bone replacement in laboratory studies.^{4,8,9} However, previous studies using DIC have used more flexible resins than polyurethane such as epoxy resin⁶ and acrylic resin¹¹ as substrate for implant installation. As DIC results are dependent on the displacement of the pixels captured by the camera, a material that does not

deform easily requires larger loads to capture visual results. This study used a bone simulator that allowed obtaining a strain pattern that could be correlated with the numerical model simulated under masticatory load value correspondent to the maximum bite force of a healthy adult man.¹⁸

An approximation of 11% was observed between the methods. This finding is in agreement with previous studies which reported that FEA generates correlated measurements, but greater than DIC.^{6,7} Both methods accounted for greater peri-implant strain around the implant located under the load application site. During the axial loading, the colorimetric strain maps was predominant blue, showing lower values of vertical and horizontal displacement, and consequently lower strain values. For non-axial loading, the last implant (distal, lever region) was more affected and the strain map patterns could be interpreted as more aggressive.

Previous studies have shown that there is a greater potential for deleterious effects in the peri-implant region when non-axial loading is applied.^{9,19,20} Therefore, the implant-supported rehabilitation should be performed by the clinician focusing on the improve of axially force transmission trough the structures. In the case of implant-supported fixed prostheses, this effect is directly associated with the number of implants involved in the masticatory load distribution and the lever arm extension.²⁰ For example, even with 3 implants splinted, the non-axial loading could modify negatively the mechanical response of the bone tissue increasing the cervical strain around the last implant. Also, this behavior of increased strain peak associated with a more aggressive pattern of stress concentration when a prosthesis is submitted to non-axial loading has already been reported and correlated with possible areas of bone resorption.^{4,9}

Following the methodologies already reported in the literature,^{6,11} the strain peaks calculated with DIC were collected from the block surface from the cervical region to five millime-

ters in the apical direction. This approach was already used to describe that the cervical area is the bone region with higher strain for 3-unit implant-supported fixed dental prosthesis,¹¹ a pattern that can be observed in the present study also. Statistical analysis demonstrated that the central implant presents similar strain values for both loadings. Thus, the lever action is sufficient to generate a peri-implant strain as strong as chewing directly on this implant. The other implants arranged at the extremities of the prosthesis behave differently in each situation. Under the axial load, both implants dissipate significantly equal amounts of the masticatory force. However, under the non-axial load, the closest implant to the load application area (implant 3) was significantly more affected. This effect in the central implant was not observed by any previous paper that used strain gauge to measure the cervical strain in the 3-unit implant-supported fixed dental prosthesis with similar load application.⁴ The authors reported that the strain gauge could present different areas of measurement in comparison with FEA because this method only show the strain in a specific region that could be different from the region of maximum magnitude in the simulation.⁴

In observing the von-Mises stress isolines generated in the implants (Figure 5), the external hexagon platform is the most affected region, suggesting greater damage in implant 3 under non-axial loading. The maximum strain value generated in implant 3 increased about 77% with the application of the non-axial load (0.22 - 0.39). This stress criteria are used to evaluate ductile solids such as titanium, and represents possible metal kneading zones and loss of determined geometric characteristics.^{4,9,21} Thus, the hexagon may have its edges rounded and the seating passivity of the prosthesis could be compromised.²² This is a concern once the osseointegrated implant is not easily replaceable such as the prosthesis itself. Damages in the implant platform can difficult or even make impossible the manufacture on future structures on it. The increase in the vertical misfit because of the plastic deformation on titanium implant platform could be a possible factor to increase the stress in the screw, to facilitate the torque loss and to increase the failure probability under fatigue.¹⁷

It is reported in the literature that the use of fixed cantilever prosthesis has a high survival rate,²³ but some complications can be observed such as marginal bone loss around the distal implant.² This suggests that any factor that potentiates the stress concentration such as long lever arms,²⁰ inclined cusps,²⁵ wide occlusal platforms,² premature occlusal contacts²⁵ different dental materials^{8,26,27} and the application of non-axial loads⁴ could facilitate stress concentration. Thus, the results demonstrate that a masticatory load with the same intensity but applied at different sites can significantly modify the mechanical behavior of the implant and the bone. In this way, greater care is needed when planning this kind of rehabilitation.

CONCLUSION

Based in this validated finite element model, the following can be concluded:

- For implant-retained cantilever fixed prosthesis the loading incidence in the lever arm are capable to induce higher bone strain and implant stress. If it is possible, cantilevered loading should be avoided as the first option to perform an rehabilitation.

ACKNOWLEDGEMENTS

The authors would like to thank São Paulo Research Foundation (FAPESP) with the grant n° 17/09104-4.

REFERENCES

1. Raes S., Raes F., Cooper L. et al. Oral health-related quality of life changes after placement of immediately loaded single implants in healed alveolar ridges or extraction sockets: a 5-year prospective follow-up study. *Clin. Oral Implants Res.*, 2017;**28**:662-667.
2. Aglietta M., Siciliano V.I., Zwahlen M. et al. A systematic review of the survival and complication rates of implant supported fixed dental prostheses with cantilever extensions after an observation period of at least 5 years. *Clin. Oral Implants Res.*, 2009;**20**:441-451.
3. Rungsiyakull C., Rungsiyakull P., Li Q., Li W., Swain M. Effects of occlusal inclination and loading on mandibular bone remodeling: a finite element study. *Int. J. Oral Maxillofac. Implants*, 2011;**26**:527-537.
4. Tribst J.P., Rodrigues V.A., Dal Piva A.O., Borges A.L., Nishioka R.S. The importance of correct implants positioning and masticatory load direction on a fixed prosthesis. *J. Clin. Exp. Dent.*, 2018;**10**:e81-e87.
5. Tribst J.P.M., Dal Piva A.M.D.O., Borges A.L.S. Biomechanical tools to study dental implants: a literature review. *Braz. Dent. Sci.*, 2016;**19**:5-11.
6. Tiozzi R., Vasco M.A., Lin L. et al. Validation of finite element models for strain analysis of implant-supported prostheses using digital image correlation. *Dent. Mater.*, 2013;**29**:788-796.
7. Berahmani S., Janssen D., Verdonschot N. Experimental and computational analysis of micromotions of an uncemented femoral knee implant using elastic and plastic bone material models. *J. Biomech.*, 2017;**61**:137-143.
8. Datte C.E., Tribst J.P., Dal Piva A.O. et al. Influence of different restorative materials on the stress distribution in dental implants. *J. Clin. Exp. Dent.*, 2018;**10**: e439-e444.
9. Tribst J.P.M., Rodrigues V.A., Borges A.L.S., Lima D.R., Nishioka R.S. Validation of a Simplified Implant-Retained Cantilever Fixed Prosthesis. *Implant Dent.*, 2018;**27**:49-55.
10. Epprecht A., Zeltner M., Benic G., Özcan M. A strain gauge analysis comparing 4-unit veneered zirconium dioxide implant-borne fixed dental prosthesis on engaging and non-engaging abutments before and after torque application. *Clin. Exp. Dent. Res.*, 2018;**4**:13-18.
11. Peixoto R.F., Macedo A.P., Martinelli J. et al. A digital image correlation analysis of strain generated by 3-unit implant-supported fixed dental prosthesis: an in vitro study. *Implant Dent.*, 2017;**26**:567-573.

12. Lee J.H., Lee W., Huh Y.H., Park C.J., Cho L.R. Impact of intentional overload on joint stability of internal implant-abutment connection system with different diameter. *J. Prosthodont.*, 2019;**28**:e649-e656.
13. Benzing U.R., Gall H., Weber H. Biomechanical aspects of two different implant-prosthetic concepts for edentulous maxillae. *Int. J. Oral Maxillofac. Implants*, 1995;**10**:188-198.
14. Rubo J.H., Capello Souza E.A. Finite-element analysis of stress on dental implant prosthesis. *Clin. Implant Dent. Relat. Res.*, 2010;**12**:105-113.
15. Sousa M.P., Tribst J.P.M., de Oliveira Dal Piva A.M., Borges A.L.S., de Oliveira S., da Cruz P.C. Capacity to maintain placement torque at removal, single load-to-failure, and stress concentration of straight and angled abutments. *Int. J. Periodontics Restorative Dent.*, 2019;**39**:213-218.
16. Alkan I., Sertgöz A., Ekici B. Influence of occlusal forces on stress distribution in preloaded dental implant screws. *J. Prosthet. Dent.*, 2004;**91**:319-325.
17. Melo Filho A.B., Tribst J.P.M., Ramos N.C. et al. Failure probability, stress distribution and fracture analysis of experimental screw for micro conical abutment. *Braz. Dent. J.*, 2019;**30**:157-163.
18. Fastier-Wooller J., Phan H.P., Dinh T. et al. Novel low-cost sensor for human bite force measurement. *Sensors (Basel)*, 2016;**16**:1-10.
19. Suedam V., Moretti Neto R.T., Sousa E.A., Rubo J.H.. Effect of cantilever length and alloy framework on the stress distribution in peri-implant area of cantilevered implant-supported fixed partial dentures. *J. Appl. Oral. Sci.*, 2016;**24**:114-120.
20. Ebadian B., Mosharraf R., Khodaeian N. Effect of cantilever length on stress distribution around implants in mandibular overdentures supported by two and three implants. *Eur. J. Dent.*, 2016;**10**:333-340.
21. Hill R. A theory of the yielding and plastic flow of anisotropic metals. *Proc. R. Soc. Lond. A.*, 1948;**193**:281-297.
22. Wang C.F., Huang H.L., Lin D.J., Shen Y.W., Fuh L.J., Hsu J.T. Comparisons of maximum deformation and failure forces at the implant-abutment interface of titanium implants between titanium-alloy and zirconia abutments with two levels of marginal bone loss. *Biomed. Eng. Online*, 2013;**12**:1-10.
23. Brignardello-Petersen R. Single implant-supported 2-unit cantilever fixed dental prosthesis seem to result in high patient satisfaction and survival up to 3 years. *J. Am. Dent. Assoc.*, 2017;**148**:e141.
24. da Fonseca G.F., Dal Piva A.M., Tribst J.P., Borges A.L. Influence of restoration height and masticatory load orientation on ceramic endocrowns. *J. Contemp. Dent. Pract.*, 2018;**19**:1052-1057.
25. Chaichanasiri E., Nanakorn P., Tharanon W., Sloten J.V. Finite element analysis of bone around a dental implant supporting a crown with a premature contact. *J. Med. Assoc. Thai.*, 2009;**92**:1336-1344.
26. Tribst J.P.M., Dal Piva A.M., Özcan M., Borges A.L.S., Bottino M.A. Influence of ceramic materials on biomechanical behavior of implant supported fixed prosthesis with hybrid abutment. *Eur. J. Prosthodont. Restor. Dent.*, 2019;**27**:76-82.
27. Tribst J.P.M., Dal Piva A.M.O., de Melo R.M., Borges A.L.S., Bottino M.A., Özcan M. Short communication: Influence of restorative material and cement on the stress distribution of posterior resin-bonded fixed dental prostheses: 3D finite element analysis. *J. Mech. Behav. Biomed. Mater.*, 2019;**96**:279-284.